Sugar Mimics: An Artificial Receptor for Cholera Toxin

Anna Bernardi,*,‡ Anna Checchia,‡ Paola Brocca,§ Sandro Sonnino,§ and Fabio Zuccotto[||]

Contribution from the Dipartimento di Chimica Organica e Industriale, Università di Milano, via Venezian 21, 20133 Milano, Italy, Dipartimento di Chimica e Biochimica Medica, Universitá di Milano, Italy, and Welsh School of Pharmacy, University of Cardiff, Cardiff, Wales, UK

Received October 9, 1998

Abstract: The paper describes the pseudosugar **2** [Galβ1−3GalNAcβ1−4(NeuAcα2−3)DCCHD], a high affinity binder of cholera toxin (CT). The molecule was designed using molecular modeling techniques to mimic the natural CT membrane receptor, ganglioside GM1. The central residue of GM1, a 3,4-disubstituted galactose unit, was recognized as the ganglioside scaffold element and substituted with a conformationally locked cyclohexanediol (DCCHD). DCCHD was synthesized in enantiopure form using enantioselective Diels Alder methodology and regioselectively α-sialylation at the equatorial position. Glycosylation with a Galβ(1−3)-GalNAc donor completed the synthesis of **2.** The solution structure of **2** and its binding ability to CT were found to be analogous to those of the GM1 oligosaccharide.

Introduction

The inhibition of carbohydrate−protein interactions is an attractive strategy to control a number of important biological phenomena which are initiated by formation of a sugar−protein complex. Although carbohydrate mimetics have been used to this end,[1] their rational design has rarely been addressed.[1,2] The complex formed by cholera toxin (CT), a hexameric protein, and its membrane receptor, the membrane glycolipid ganglioside GM1 **1**, is regarded as a paradigm in the study of sugar−protein interactions. In this paper we report on the use of computational tools for the rational design of a pseudosugar mimic of GM1. The pseudosugar **2**, which contains the novel conformationally constrained diol **3** as a 3,4-disubstituted galactose mimic, was found to exhibit the same three-dimensional structure of GM1 oligosaccaharide and to be a potent inhibitor of the interaction of GM1 with CT. The methodology presented here, as well as diol **3**, may have wider applications in the study of protein−sugar interactions.

The sialic acid-containing glycolipids of cell membranes are implicated in a number of cellular signaling events, and function as binding sites for various toxins, hormones, and viruses.[3] The specific membrane receptor of the bacterial toxins CT and heat-labile toxin of *Escherichia coli* (LT) is the pentasaccharide portion of ganglioside GM1 [Galβ1−3GalNAcβ1−4(NeuAcα2−3)Galβ1−4Glcβ1−1Cer] **1**. LT and CT are 80% homologous AB_5 hexameric proteins: actual cell intoxication is carried out by a catalytic fragment of the A subunit, while the B_5 pentamer performs recognition of and anchoring to the cell membrane. The interaction of GM1 with LT and CT has been fully characterized.[4−6] Biochemical[5] and structural[6] data indicate that

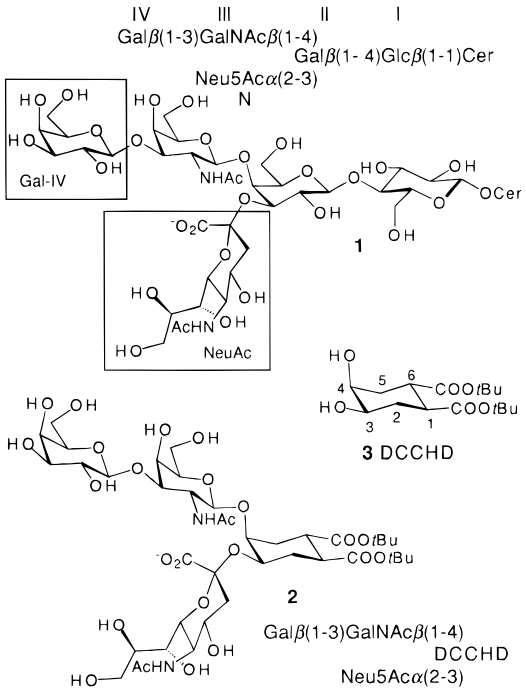

Figure 1. Structures of ganglioside GM1, **1**, its designed mimic **2**, and the conformationally restricted dicarboxy cyclohexanediol (DCCHD) **3**. The binding determinants of **1** are highlighted in the boxes.

the two sugars at the nonreducing end of GM1, galactose (Gal-IV) and sialic acid (NeuAc) (see Figure 1), are essential for binding. In particular, the structure of the CT:GM1 complex[6a,b] shows that the GM1 pentasaccharide binds with a two-finger

‡ Dipartimento di Chimica Organica e Industriale.
§ Dipartimento di Chimica e Biochimica Medica.
|| University of Cardiff.

(1) *Topics in Current Chemistry*; Driguez, H., Thiem, J., Eds.; Springer-Verlag: Berlin, 1997; Vol. 187; *Carbohydrate Mimics: Concepts and Methods*; Chapleur, Y., Ed.; Wiley-VCH: New York, 1998.
(2) Kolb, H. C.; Ernst, B. *Chem. Eur. J.* **1997**, *3*, 1571−1578.
(3) Hakomiri, S.-I. *Biochem. Soc. Trans.* **1993**, *21*, 583−585.
(4) Spangler, B. D. *Microbiol. Rev.* **1992**, *56*, 622−647 and references therein. Masserini, M.; Freire, E.; Palestini, P.; Calappi, E.; Tettamanti, G. *Biochemistry* **1992**, *31*, 2422−2426.
(5) Lanne, B.; Schierbeck, B.; Karlsson, K. A. *J. Biochem.* **1994**, *116*, 1269−1274; Fukuta, S.; Magnani, J. L.; Twiddy, E. M.; Holmes, R. K.; Ginsburg, V. *Infect. Immun.* **1988**, *56*, 1748−1753; Ångstrøm, J.; Tenenberg, S.; Karlsson, K. A. *Proc. Natl. Acad. Sci. U.S.A.* **1994**, *91*, 11859−11863; Schengrund, C.-L.; Ringler, N. J. *J. Biol. Chem.* **1989**, *264*, 13233−13237.
(6) (a) Merritt, E. A.; Sarfaty, S.; v. d. Akker, F.; L'Hoir, C.; Martial, J. A.; Hol, W. G. J. *Protein Sci.* **1994**, *3*, 166−175. (b) Merritt, E. A.; Sarfaty, S.; Jobling, M. G.; Chang, T.; Holmes, R. K.; Hirst, T. R.; Hol, W. G. J. *Protein Sci.* **1997**, *6*, 1516−1528. (c) Merritt, E. A.; Hol, W. G. J. *Curr. Opin. Struct. Biol.* **1995**, *5*, 165−171 and references therein.

10.1021/ja983567c CCC: $18.00
Published on Web 03/02/1999

grip: the large majority of interactions between the receptor and the toxin involve Gal-IV and NeuAc, with a limited contribution from the *N*-acetylgalactosamine (GalNAc) residue (see Figure 1). A computational model of the LT:GM1 complex which was a fair reproduction of the CT:GM1 X-ray structure was obtained using a Monte Carlo/energy minimization (MC/EM) conformational search of the sugar within the toxin binding pocket.[7]

NMR data[8] and MC/EM calculations[9] for GM1 in water solution have revealed that its pentasaccharide is significantly conformationally restricted. In particular the core trisaccharide GalNAcβ1−4(NeuAcα2−3)Galβ was found to exist mainly in a single conformation, which closely resembles the bound conformation observed by X-ray crystallography. The Galβ1−3GalNAc anomeric bond is only slightly more flexible, and the NOE contacts observed around it can be interpreted as arising from either two[8] or one "average"[9] conformations. The overall picture is that of a highly preorganized receptor for toxin binding. Very likely, the loss of conformational freedom in GM1 results from the 3,4-branching at Gal-II (Figure 1);[10−12] thus this residue, which does not interact with the protein, appears to act as a scaffold and hold Gal-IV and NeuAc in the required position. The GM1 mimic **2** was designed based on this hypothesis by retaining the ganglioside binding determinants and replacing the scaffold element with an appropriate diol, designed to reproduce the topological features of a 3,4-disubstituted galactose.

Materials and Methods

Materials. GM1 ganglioside was prepared[13] from the total ganglioside mixture extracted from calf brain.[14] The penta-oligosaccharide of GM1 was obtained by ozonolysis of GM1, followed by alkaline hydrolysis.[15]

Computational. All calculations were run with MacroModel 4.5,[16] using the AMBER* force field with MNDO-derived parameters for NeuAc[9] and following previously established MC/EM protocols.[7,9] Twenty thousand MC/EM steps were performed both for the complex and isolated **2**. Bulk water solvation was simulated using MacroModel's generalized Born GB/SA continuum solvent model.[17] Previous studies[7] had shown that under these conditions the crystal structure of the CT:GM1 complex was best reproduced when five crystallographic water molecules were retained. Of these, three are located outside the protein binding site and solvate the carboxy group of Glu-51. The other two molecules, at crystallographic solvation sites 2 and 3, mediate specific interactions between the sugar and the protein. These molecules were consistently found in a set of five different structures of LT, CT, and their sugar complexes[6c] and were likewise included in the calculation of the LT:**2** complex.

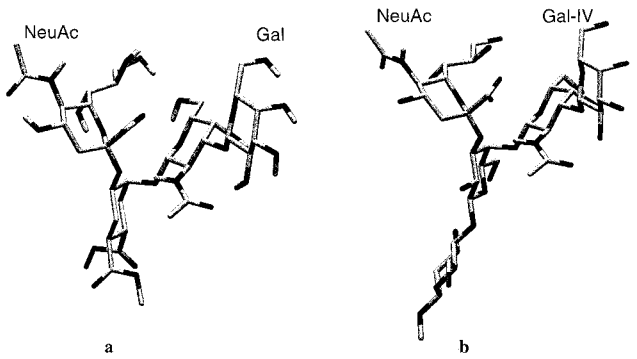

Figure 2. (a) Lowest energy conformation of **2**. (b) Solution conformation of GM1 **1** (from refs 8 and 9).

NMR. ROESY experiments[26] were conducted applying a spin lock pulse of 2.6 kHz strength at one end of the spectrum to avoid scalar transfer.[8,18] For the experiments in D_2O, mixing time was varied between 150 and 220 ms and the temperature in the range 303−313 K. For the experiments in DMSO, mixing time was varied between 180 and 230 ms and the temperature in the range 303−318 K. Spectral assignments are reported as Supporting Information.

Inhibition of the GM1:CT Formation. Binding of **2** to CT was investigated by measuring the inhibition of GM1:CT formation.[19] In parallel experiments GM1 oligosaccharide was used. Each well of a 96-well microtiter plate (Greiner) was covered with 0.5 μg of GM1 dissolved in 50 μL of 95% ethanol. After overnight drying at room temperature the wells were incubated for 2.5 h with 250 μL of 1% albumin in 0.05 M PBS (sodium phosphate buffer, pH 7.4, 9% NaCl). After removal of the solution, the wells were washed five times with 0.05 M PBS and incubated for 2.5 h with 50 μL of 1% albumin in 0.05 M PBS containing 0.2 μg of *Vibrio cholerae* toxin B subunit conjugated to horseradish peroxidase (Sigma) preincubated for 2.5 h with increasing amounts of GM1 oligosaccharide or **2**. The CT solution was discarded, the wells were washed five times with 250 μL of 0.05 M PBS, and 50 μL of a 0.04% solution of *o*-phenyldiammine in 0.02 M citrate/phosphate buffer (pH 5) and 17 μL of H_2O_2 were added. After 20 min in the dark, 50 μL of H_2SO_4 were added to block the reaction, and the color intensity was determined by spectrophotometry.

Results and Discussion

After the central 3,4-disubstituted Gal-II unit of GM1 was recognized as the ganglioside scaffold element, the design of a structural and functional analogue was sought using an appropriate conformationally locked *cis*-1,2-cyclohexanediol to replace it. One such molecule is the dicarboxy cyclohexanediol **3** (DCCHD), which possesses the same absolute and relative configuration of natural galactose and is locked in a single chair conformation. Indeed, MM3* calculations show that the chair conformation of DCCHD depicted in Figure 1 is 3.2 kcal mol^{-1} more stable than the chair which features trans diaxial carboxy groups.

Based on the above considerations, the pseudo-tetrasaccharide **2**, which retains the Gal and NeuAc recognition determinants and uses **3** as the scaffold element, was devised as an artificial receptor for LT and CT. Conformational analysis of **2** was performed both for the isolated molecule and in the binding pocket of LT, and the predicted three-dimensional structures were compared to those of GM1.

(7) Bernardi, A.; Raimondi, L.; Zuccotto, F. *J. Med. Chem.* **1997**, *40*, 1855−1862.
(8) Acquotti, D.; Poppe, L.; Dabrowski, J.; v. d. Lieth, C.-W.; Sonnino, S.; Tettamanti, G. *J. Am. Chem. Soc.* **1990**, *112*, 7772−7778.
(9) Bernardi, A.; Raimondi, L. *J. Org. Chem.* **1995**, *60*, 3370−3377.
(10) Both the unbranched carbohydrates asialo-GM1 (ref 11) and GM4 (NeuAc(α2,3)Gal-βOMe) (ref 12) were shown to be considerably more flexible than GM1 by NMR spectroscopy.
(11) Scarsdale, N. J.; Prestegard, J. H.; Yu, R. K. *Biochemistry* **1990**, *29*, 9843−9855 and references therein.
(12) Poppe, L.; Dabrowski, J.; v. d. Lieth, C.-W.; Numata, M.; Ogawa, T. *Eur. J. Biochem.* **1989**, *180*, 337−342.
(13) Acquotti, D., Cantú, L., Ragg, E.; Sonnino, S. *Eur. J. Biochem.* **1994**, *225*, 271−288
(14) Tettamanti, G.; Bonali, F.; Marchesini, S.; Zambotti, V. *Biochim. Biophys. Acta* **1973**, *296*, 160−170
(15) Wiegandt, H.; Bucking, H. W. *Eur. J. Biochem.* **1970**, *15*, 287−292.
(16) Mohamadi, F.; Richards, N. G. J.; Guida, W. C.; Liskamp, R.; Lipton, M.; Caufield, C.; Chang, G.; Hendrickson, T.; Still, W. C. *J. Comput. Chem.* **1990**, *11*, 440−467.
(17) Still, W. C.; Tempzyk, A.; Hawley, R.; Hendrickson, T. *J. Am. Chem. Soc.* **1990**, *112*, 6127−6129.
(18) Farmer, H. B. T.; Macura, S.; Brown, L. R. *J. Magn. Res.* **1987**, *72*, 347−352.
(19) Wu, G.; Leeden, R. *Anal. Biochem.* **1988**, *173*, 368−375; Carpo, M.; Nobile-Orario, E.; Chigorno, V.; Sonnino, S. *Glycoconjugate J.* **1995**, *12*, 729−731.

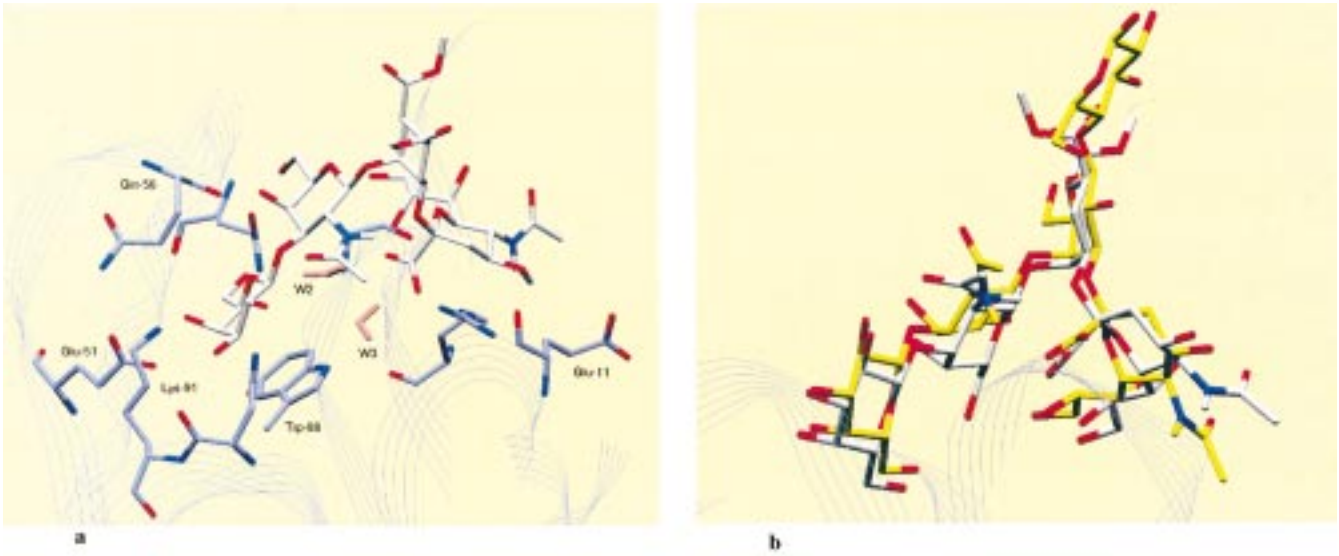

Figure 3. (a) Minimum energy conformation of the LT:**2** complex as calculated by MC/EM. LT in blue; **2** in white; the two water molecules in pink are crystallographic water molecules from the LT crystal structure that are conserved in the calculations (see ref 7). (b) Superimposition of the calculated LT:**2** complex with the X-ray structure of CT:GM1. The picture was obtained by sumperimposing three binding-site residues conserved in LT and CT (Glu-51, Lys-91, and Trp-88). LT was deleted for clarity. CT in blue; **2** in white; GM1 **1** in yellow.

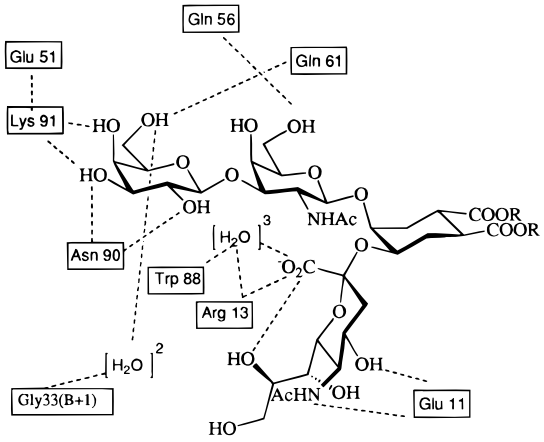

Figure 4. Map of the interactions of **2** with LT, as calculated in the global minimum of the MC/EM search.

The conformational search of isolated **2** was run simulating water solvation with the GB/SA model and yielded 10 conformers within 1 kcal mol^{-1} from the global minimum. They all shared the common conformation of the branched pseudo-trisaccharide fragment shown in Figure 2a. Comparison of the global minimum with the NMR solution structure of GM1[8] (Figure 2b) clearly shows that DCCHD holds the terminal Gal and NeuAc in the same relative position as the native galactose.

The analysis of the LT:**2** complex was also very promising, and yielded low energy conformations which featured all the expected sugar−protein contacts[6] (see global minimum in Figure 3a). A map of the interactions of **2** with LT, as seen in the global minimum of the MC/EM search is reported in Figure 4**.** The corresponding maps for GM1:CT and GM1:LT as seen by X-ray crystallography (from ref 6a) or calculated by molecular mechanics (from ref 7) are reported as Supporting Information. The main difference between the calculated contacts in LT: **2** and those observed in GM1:CT is the absence in the former of interactions between the NeuAc side-chain and the water molecule at crystallographic solvent site 2 (W2 in Figure 3a). A visual comparison of the lowest energy conformation of LT:**2** and the X-ray structure of CT:GM1 was obtained by superimposing three active-site residues of LT and CT. The resulting picture is reported in Figure 3b and shows that **2** and GM1 are expected to adopt a common disposition in the toxin binding pocket. The root-mean-square deviation (rmsd) for equivalent residues of the sugar substrates are collected in Table 1. The buried surface area of the protein binding site in the lowest-energy conformation of the LT:**2** complex was calculated to be 347 Å^2, which compares favorably with the experimental value of 403 ± 10 Å^2 for the CT:GM1 complex.[20]

On this basis, the synthesis of **2** was undertaken and performed as outlined in Scheme 1.[21] Enantiopure **3**[21] was synthesized using Helmchen's stereoselective Diels−Alder methodology,[22,23] followed by functional group manipulation and cis-dihydroxylation ($OsCl_3$, Me_3NO) of the cyclohexene double bond. Regioselective α-sialylation[24] of **3** with the phosphite **4**[25] (TMSOTf, EtCN, −40°, 50% yield, based on reacted **3**) followed by glycosylation with the Galβ(1−3)-GalNAc donor **5** (TMSOTf, refluxing CH_2Cl_2, 30% yield) completed the synthesis of **2**.

Two-dimensional 500-MHz ROESY[26] spectra of **2** were obtained in D_2O and DMSO-d_6 solution. The observed inter-residual contacts and corresponding NOE distances are collected in Table 2 and compared with the computational prediction and the data reported in the literature for GM1 in DMSO-d_6.[8]

The conformational restriction of the core trisaccharide in GM1 results in a very characteristic set of NOE contacts. Typically, a strong cross-peak is observed between the H3 of Gal-II (II-3) and the 3-axial proton of NeuAc (N-3ax) (Table 2, entry 1). The GalNAc anomeric proton (III-1) shows a single

(20) Merritt, E. A.; Sarfaty, S.; Feil, I. K.; Hol W. G. J. *Structure* **1997**, *5*, 1485−1499 and references therein.

(21) Analytical data for compounds **2** and **3** are given in the Supporting Information. Details of the synthetic procedure will be reported elsewhere.

(22) Hartmann, H.; Hady, A. F. A.; Sartor, K.; Weetman, J.; Helmchen, G. *Angew. Chem., Int. Ed. Engl.* **1987**, *26*, 1143−1144. The desired (*S*,*S*)-diacid was obtained as a 6:1 mixture with the (*R*,*R*)-enantiomer and purified via crystallization of its quinine salt, following a published procedure (ref 23).

(23) Walborsky, H. M.; Barash, L.; Davis, T. C. *Tetrahedron* **1963**, *19*, 2333−2351.

(24) Okamoto, K.; Goto, T. *Tetrahedron* **1990**, *17*, 5835−5857.

(25) Martin, T. J.; Schmidt, R. R. *Tetrahedron Lett.* **1992**, *33*, 6123−6126; Martin, T. J.; Brescello, R.; Toepfer, A.; Schmidt, R. R. *Glycoconj. J.* **1993**, *10*, 16−25.

(26) Bax, A.; Davis, D. G. *J. Magn. Res.* **1985**, *64*, 533−535.

Table 1. Superimposition between the X-ray CT:GM1 Structure and the LT:**2** Complex. Rms Deviations[a]

					NeuAc side chain					
residue	Gal-IV	GalNAc	Gal-II/DCCHD	NeuAc	C7	C8	C9	O7	O8	O9
rmsd[b] (Å)	0.495	0.815	0.252	0.587	1.129	1.154	1.560	1.117	1.241	1.755

[a] As obtained by superimposing Glu-51, Lys-91, and Trp-88 side chains. The lowest minimum conformation was used for the LT:**2** complex. [b] Rms deviations of sugar residues were measured between ring centroids.

Table 2. Experimental and Calculated Inter-residual Contacts for **2** (Å)

entry	contacts[a]	calcd distance[b]	NOE distance (D_2O)	NOE distance (DMSO-d_6)	NOE distance in GM1[c] (contact)
1	N-3ax/CHD-3	2.3	2.5	2.3	2.1 (N-3ax/II-3)
2	N-8/GN-1	2.9	*d*	*d*	3.1 (N-8/III-1)
3	N-8/CHD-4	2.6	4.5	2.8	*e* (N-8/II-4)
4	N−OH8/GN-1	3.1		3.0	2.6 (N−OH8/III-1)
5	N−OH8/CHD-3	5.4		4.1	*e* (N−OH8/II-3)
6	GN-1/CHD-4	2.3	2.2	2.2	2.2 (III-1/II-4)
7	GN−Ac/CHD-2ax	3.2	*d*	*e*	3.1 (III−Ac/II-2)
8	G-1/GN-2	4.0	3.6	3.6	3.5 (IV-1/III-2)
9	G-1/GN-3	2.4	2.2	2.3	2.5 (IV-1/III-3)
10	G-1/GN-4	4.0	3.5	3.6	3.5 (IV-1/III-4)
11	G-1/GN−NH	3.4		3.4	3.5 (IV-1/III-NH)

[a] Abbreviations: N: NeuAc; CHD: DCCHD; GN: GalNAc; G: Gal. DCCHD numbering as reported in Figure 1. [b] The distances were calculated as $r = \langle r^{-6}\rangle^{-1/6}$ were $\langle r^{-6}\rangle$ is the Boltzmann average of the r^{-6} of all the individual conformations found within the first 3 kcal mol^{-1} from the global minimum (86 conformations). [c] DMSO-d_6 solution, from ref 8. [d] Not measurable, due to signal overlap. [e] No cross-peak detected.

Scheme 1. Synthesis of **2**[a]

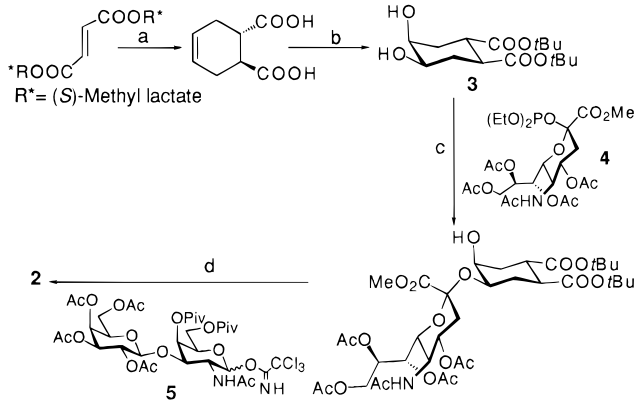

[a] a. $TiCl_4$, butadiene, CH_2Cl_2, −50 °C; LiOH. b. DMF-di-*tert*-butylacetal, refluxing benzene; $OsCl_3$, Me_3NO. c. TMSOTf, EtCN, −40 °C, then **4**; d. TMSOTf, CH_2Cl_2, 40 °C, then **5**; cat. MeONa, MeOH, then H_2O.

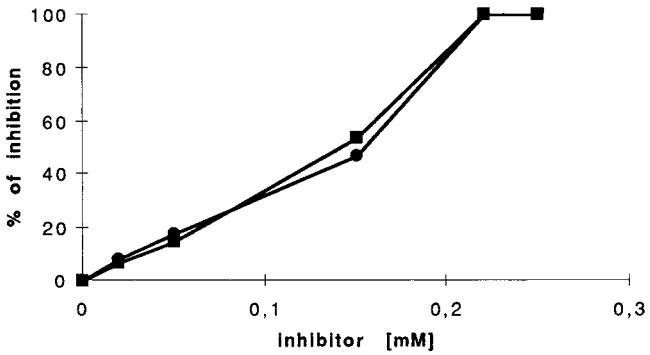

Figure 5. Inhibition of the GM1:CT binding in ELISA by the GM1 pentasaccharide (●) and **2** (■). Standard deviation of data determined on 4 experiments was ±30%. Over a concentration of 200 μg/mL inhibition was always 100%, for both **2** and the pentasaccharide. Each microtiter well was covered with 1 μg of GM1. Peroxidase conjugate CT B subunit was used at 1.75 μg/mL.

transglycosidic contact with the H4 proton of Gal-II (II-4) (Table 2, entry 6), and gives two cross-peaks with the H8 and OH8 protons of NeuAc (N-8 and N−OH8) (Table 2, entries 2 and 4). This pattern of contacts is consistent with a single dominant conformation for both the glycosidic NeuAcα2−3Gal and GalNAcβ1−4Gal bonds. The conformation of the Galβ1−3GalNAc linkage is defined by the NOE contacts observed for the anomeric proton of Gal-IV (IV-1, Table 2, entries 8−11), which shows cross-peaks of equal intensity with the H3, the H4, and the NH protons of GalNAc. The resulting three-dimensional picture of GM1 is reported in Figure 2b.[8] The ROESY spectra of **2** showed an equivalent pattern of inter-residual contacts, and the corresponding NOE distances were found to be very similar to those observed for GM1. The cross-peaks and the NOE distances observed for the galactose anomeric proton (G-1) of **2** are almost identical to those seen in GM1 (Table 2, entries 8−11). A strong cross-peak also appears between the NeuAc-3ax proton and the H3 of DCCHD (N-3ax/CHD-3, Table 2, entry 1), equivalent to the N3ax/II-3 contact in GM1. The contact between NeuAc H8 and the anomeric proton of GalNAc (N-8/GN-1) cannot be ascertained due to spectral overlap (Table 2, entry 2), but the presence of the N−OH8/GN-1 cross-peak (Table 2, entry 4) indicates proximity of the NeuAc side chain and the GalNAc residue. Furthermore, the spectra of **2** in DMSO show a cross-peak between N-8 and the H4 proton of DCCHD (N-8/CHD-4; Table 2, entry 3), which is, in turn, in proximity of GN-1 (Table 2, entry 6).[27] The main difference in the spectral patterns of **1** and **2** is the III-Ac/II-2 cross-peak observed for **1**, which is not paralleled by an equivalent contact between the acetyl protons of GalNac and the H2ax proton of DCCHD in **2** (GN-Ac/CHD-2ax; Table 2, entry 7). However, NMR analysis of **2** shows a remarkable similarity to GM1, and clearly supports the hypothesis that the two molecules share a common conformation of the binding determinants.

The computational values of the interproton distances (first column in Table 2) were calculated as Boltzmann averages over all of the conformers included in the first 3 kcal mol^{-1} from the global minimum (86 conformers). They reproduce the NOE-derived distances fairly well, thus validating the computational procedure and the three-dimensional model of **2** reported in Figure 2a.

(27) The N-8/CHD-4 cross-peak is much weaker in D_2O solution, which may suggest a different distribution of the H-bonding network for the NeuAc side chain of **2** in the two solvents.

Binding of **2** to CT was investigated by inhibiting the GM1:CT interaction in ELISA and TLC overlay assays, using previously published procedures.[19] The ELISA inhibition profiles of **2** and of the GM1 pentasaccharide are reported in Figure 5, and they are clearly overlapping. This result establishes **2** as the strongest artificial monovalent CT binder reported thus far.[20]

In conclusion, the computational tools developed for the study of GM1 and its toxin complexes[7,9] were shown to have predictive value for the design of a potent CT binder. More generally, the conformationally locked diol **3** was shown to be an effective mimic of a 3,4-disubstituted galactose and may have a wider use in the construction of pseudo-oligosaccharides featuring 3,4-Gal branching.

Acknowledgment. This work was supported by funding from the Ministero dell'Universitá e della Ricerca Scientifica e Tecnologica (MURST) and the Consiglio Nazionale delle Ricerche (CNR).

Supporting Information Available: Analytical data for compounds **2** and **3**, maps of the sugar toxin contacts in LT:**2**, LT:GM1 and CT:GM1 (PDF). This material is available free of charge via the Internet at http://pubs.acs.org.

JA983567C